# 341. Research of nonlinear electromechanical and vibro-impact interactions in electrostatically driven microactuator

**R. Dauksevicius[1], V. Ostasevicius[2], R. Gaidys[3]**
[1,2,3] Kaunas University of Technology,
K. Donelaicio 73, LT-44029, Kaunas, Lithuania
**E-mail:** [1]*rolanasd@centras.lt*, [2]*vytautas.ostasevicius@ktu.lt*, [3]*rimvydas.gaidys@ktu.lt*

*(Received 22 January 2008; accepted 20 March 2008)*

**Abstract:** This paper provides results of dynamic numerical analysis of nonlinear electromechanical and vibro-impact interactions in electrically-actuated contact-type microactuator, which is a common component in such devices as microswitches. Mathematical modeling was performed by means of finite element method, representing microactuator as a 3D cantilever microstructure and taking into account influence of bending forces generated by electrostatic field, damping forces due to squeezed air-film in the gap as well as bouncing of the microactuator tip upon its contact with substrate. Electrostatic-structural simulations were performed in order to predict actuation (pull-in) voltages of fabricated microswitches as well as to study influence of various system parameters on the value of the voltage. Results of these simulations were compared with experimental findings obtained by using electrical probe measurements of fabricated microswitches. Numerical analysis of free impact vibrations was carried out and allowed determination of effect of ambient air pressure and intermolecular adhesive interactions on the phenomenon of contact bouncing.

**Keywords:** MEMS, microswitch, pull-in voltage, squeeze-film damping, vibro-impact, contact bounce, stiction, adhesion.

## Introduction

Microelectromechanical systems (MEMS) refer to microscopic devices that have a characteristic length of less than 1 mm but more than 1 μm and combine electrical and mechanical components. One of the core technologies used for MEMS manufacturing is surface micromachining, which is the fabrication of microstructures from deposited thin films. Major actuation and sensing methods encountered in MEMS are: piezoresistive, piezoelectric, thermal, electromagnetic, optic and electrostatic. The latter is the most common method due to relatively easy fabrication and fairly simple structure of electrostatic microdevices [1]. Many traditional electrostatic MEMS devices do not include contacting surfaces. However in recent years there is an increasing interest in MEMS devices possessing contact as part of their normal mode of operation. Among such devices, the fast development of MEMS switches is very promising. They offer significant advantages over their solid-state and conventional electromechanical counterparts including high linearity, low insertion loss and power consumption, small size, wider frequency range, good isolation, and relatively low cost. However, wider commercial availability of MEMS switches is still hindered today because of drawbacks related to higher actuation voltages, lower switching speed, and insufficient long-term reliability. The latter is one of the most critical issues [2]. Interrelated parasitic effects of contact bounce and stiction are one of the major reasons that degrade reliability of microswitches [2-9]. Due to the elastic response of contacting microstructure, at each on/off cycle, its tip bounces over the substrate a number of times upon contact, as have been already described by K. Petersen in 1979 [10]. This effect is not unexpected, since these switches are essentially a microscopic copy of mechanical relays, in which contact bounce is a well-known phenomenon [11,12]. Contact bounce in switches is harmful since it induces a severe damage of the

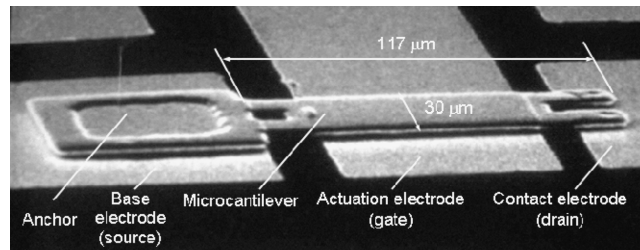


(a)

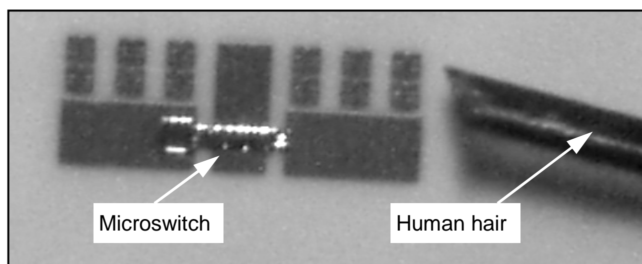


(b)

**Fig. 1.** (a) Scanning electron microscope (SEM) image of surface-micromachined electrostatically-actuated microswitch fabricated at KTU, (b) general view of the microswitch in comparison to the size of a human hair

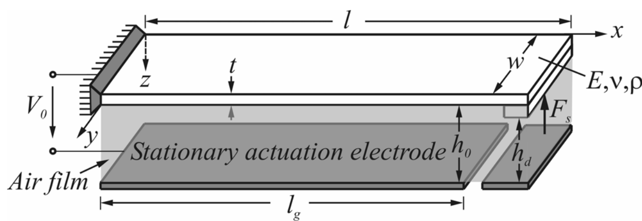


**Fig. 2.** Schematic of electrostatically-actuated cantilever microstructure under the effect of squeeze-film damping including adhesive-repulsive contact force $F_s$.

tip/substrate interface by mechanical hammering and electrical arching, thus favoring the initiation and subsequent propagation of subsurface cracks, facilitating material transfer upon beam detachment. Such a progressive degradation of the tip/substrate interface can eventually lead to so-called stiction and make the microswitch non-functional [3].

Stiction (a contraction for 'static friction') is usually defined as unintentional permanent attachment of compliant microstructure surfaces occurring during contact when restoring forces are unable to overcome adhesive interfacial forces [13-15]. Many researchers involved in modeling and experimental study of microswitch-related phenomena emphasize that a deeper understanding is required in the field of vibro-impact interactions [2-9]. Consequently, to improve the mechanical reliability of microswitches, besides a correct selection of the interfacial materials [16], it is of fundamental importance to model and analyze vibro-impact dynamics taking into account also microscale-specific contact effects related to surface interactions (i.e. adhesion).

## Overview of investigated microdevice

Electrostatically actuated resistive-type MEMS switch (Fig. 1) has been developed and fabricated at Kaunas University of Technology. Contacting element of the microswitch is a cantilever microstructure, which is bimetal and is made of upper layer of nickel and lower layer of gold with total thickness of about 2 μm. The width of the microstructure is 30 μm and length ranges from 67 to 117 μm. Spacing between the microstructure and contact electrode (drain) is 1÷2 μm. Upon application of voltage to actuation electrode (gate), the cantilever microstructure is pulled down by the electrostatic force and the tip of the cantilever approaches and contacts the drain closing an external circuit and allowing the current to flow. When the gate voltage is removed, the restoring force of the microstructure returns it to its original position.

The aim of the current research work is to create a comprehensive finite element model of the microswitch that would accurately predict the dynamic behavior of the microdevice by accounting for several most important characteristic phenomena of different physical nature including electromechanical coupling (electrostatic-structural interaction), squeeze-film damping (viscous air damping) and contact bouncing (vibro-impact interactions). The latter has also to take into account microscale-dominant intermolecular adhesive interactions.

Table 1. Parameters of simulated microswitch.

| Description and Symbol | Value | Unit |
|---|---|---|
| Microstructure length $l$ | 117 | [μm] |
| Microstructure width $w$ | 30 | [μm] |
| Microstructure thickness $t$ | 2.0 | [μm] |
| Gate length $l_g$ | 117 | [μm] |
| Gap $h_0$ | 2.0 | [μm] |
| Tip gap $h_d$ | 0 | [μm] |
| Young's modulus $E$ | 207 | [GPa] |
| Density $\rho$ | 8908 | [kg/m$^3$] |
| Poisson's ratio $\nu$ | 0.31 | - |
| Dynamic viscosity of air $\mu$ | $18.3\times10^{-6}$ | [Pa s] |

## Modeling of vibro-impact interactions

Small-scale contacts behave fundamentally different than their large-scale counterparts and one of the most important reasons for this change in behavior is the influence of adhesion, which plays an important role in the system response of MEMS devices [13,17,18]. Due to low stiffness, large surface-to-volume ratio and small distance to adjacent surfaces of microdevices, high interfacial attractive (adhesive) forces often lead to stiction, which is one of the most common MEMS failure mechanisms [13-15,18]. Van der Waals forces are the most dominant adhesive forces in the case of smoother surfaces under dry environments, which is the case of most MEMS applications [19]. However, only recently it has been proven unambiguously that for MEMS: (a) at small roughness values, adhesion is caused mainly due to the van der Waals dispersion forces acting across extensive non-contacting areas; (b) at large roughness values, van der Waals forces at contacting asperities become the dominating contributor to the adhesion [18]. Van der Waals interaction energy between two flat surfaces is [20]:

$$\Gamma = -\frac{A_H}{12\pi D^2} \,. \tag{1}$$

Its first spatial derivative is adhesive van der Waals force per unit area:

$$F = \frac{A_H}{6\pi D^3} \,. \tag{2}$$

And van der Waals force per given contact area $A_c$ is:

$$F_c = \frac{A_H A_c}{6\pi D^3} = \frac{C_{vdW}}{D^3} \,. \tag{3}$$

where $D$ – surface roughness. $A_H$ – Hamaker constant, which characterizes van der Waals attraction of solids across a liquid or gas (typically it is assumed to be about $1 \times 10^{-19}$ J, but for interactions between metals its theoretical values calculated from Lifshitz theory is about $4 \times 10^{-19}$ J [20]).

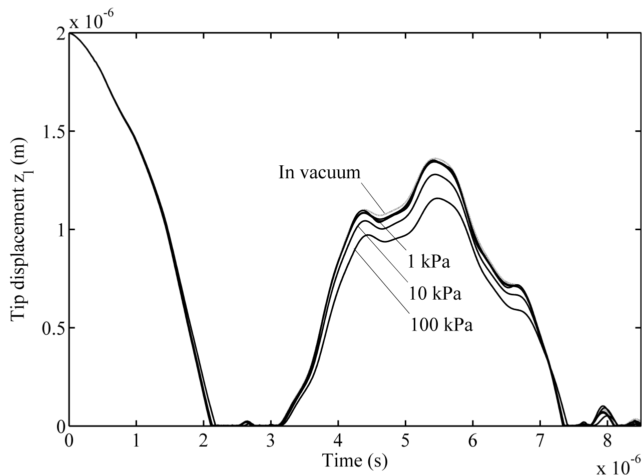


**Fig. 3.** Free impact vibrations both in vacuum and in air at pressure $p_0$ ($C_{vdW} = 10^{-30}$ Nm$^3$).

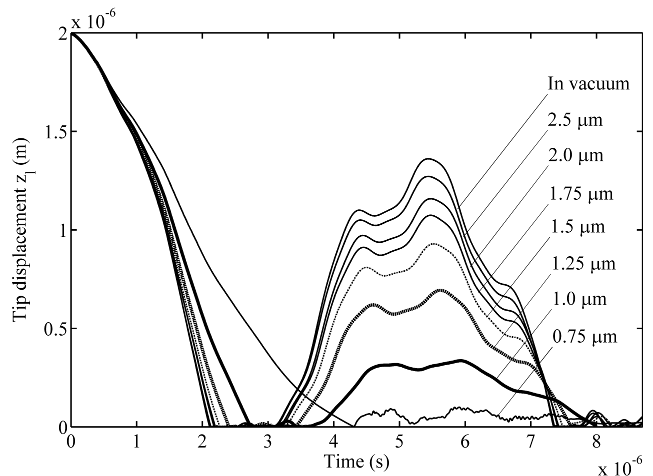


**Fig. 4.** Free impact vibrations for different $h_0$ both in vacuum and in air at pressure $p_0 = 100$ kPa ($C_{vdW} = 10^{-30}$ Nm$^3$).

In order to numerically analyze contact bouncing effects a contact model was developed that takes into account both impact interactions and influence of adhesion between tip of cantilever microstructure and drain. Tip-drain interaction is modeled by a very general adhesive-repulsive contact model, whose adhesive contribution is represented by attractive van der Waals force component and the repulsive contribution is described by a classical linear spring-like force. The adhesive-repulsive contact model is implemented in the commercially-available finite-element (FE) software Comsol [21] by representing it as a shear force $F_s(t)$ that is applied on the lower edge of free end of the microstructure (tip)(Fig. 2):

$$F_s(t) = \begin{cases} \dfrac{C_{vdW}}{[h_d - z_L(t)]^3} & for\ z_L(t) < h_d - \xi_0 \\ \dfrac{C_{vdW}}{\xi_0^3} - k[z_L(t) - (h_d - \xi_0)] & for\ z_L(t) \ge h_d - \xi_0 \end{cases} \quad (4)$$

where $h_d$ - thickness of gap between the tip of cantilever microstructure and drain; $\xi_0$ is the interatomic distance at equilibrium at the interface between tip and drain; $z_L(t)$ - displacement of the tip of cantilever microstructure.

Thus, in the presented adhesive-repulsive contact model tip-drain interaction is modeled: (a) before contact ($z_L(t) < h_d - \xi_0$) - by attractive van der Waals force component that is proportional to parameter $C_{vdW} = A_h A_c / 6\pi$ and decays with the third power of the separation distance (b) upon contact ($z_L(t) \ge h_d - \xi_0$) - by additional repulsive linear elastic force that is proportional to spring constant $k$ and grows linearly with the penetration distance.

## Modeling of electromechanical coupling

One of the most important performance parameters characterizing a microswitch is its pull-in voltage and pull-in time. In order to determine these parameters a FE model was built within Comsol that couples deformations of elastic microstructure with applied electric field. The complexity of this interaction is associated with moving boundaries during operation. In order to solve problems involving moving boundaries, the arbitrary Lagrangian-Eulerian (ALE) method is applied. The model solves the following electrostatic equation in the air domain surrounding the microstructure using ALE technique to account for air geometry changes associated with the microstructure deformation [21]:

$$-\nabla \cdot (\varepsilon \nabla V) = 0 . \quad (5)$$

where $V$ – electric potential, $\varepsilon$ - permittivity.

In this model the cantilever microstructure is placed in air-filled chamber that is electrically insulated. For the insulated surfaces of the chamber we apply boundary condition $\mathbf{n} \cdot \mathbf{D} = 0$, which specifies that the normal component of the electric displacement ($\mathbf{n} \cdot \mathbf{D}$) is zero. Bottom side of chamber has an electrode that is grounded therefore its boundary condition is $V = 0$. The microstructure is coated with a thin conductive layer from the lower side (electrode), which is placed at a positive potential therefore its boundary condition is $V = V_0$, which specifies the voltage $V_0$ connected to this electrode (Fig. 2). An electrostatic force generated by an applied potential difference between the two electrodes makes the microstructure to bend towards the grounded electrode below it. The force density that acts on the electrode of the microstructure results from the Maxwell's stress tensor [21]:

$$F_{es} = -\frac{1}{2}(\mathbf{E} \cdot \mathbf{D})\mathbf{n} + (\mathbf{n} \cdot \mathbf{E})\mathbf{D}^T . \quad (6)$$

where $\mathbf{E}$ and $\mathbf{D}$ are the electric field and electric displacement vectors, respectively, and $\mathbf{n}$ is the outward normal vector of the boundary. As the microstructure bends, the geometry of the air changes, thus continuously changing the electric field between the electrodes. And the

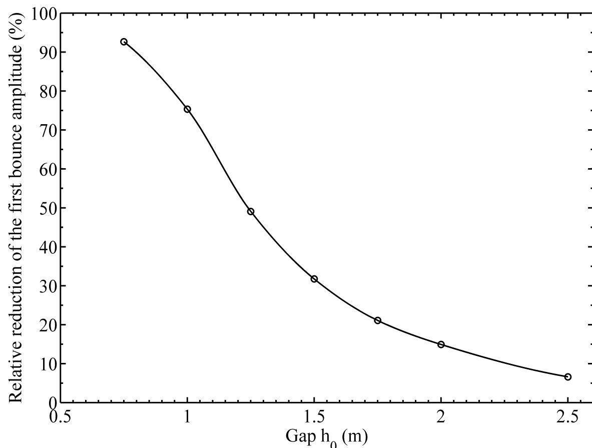


**Fig. 5.** Relative reduction of the first bounce amplitude $z_{max}$ (with respect to value obtained under vacuum conditions) presented as a function of $h_0$ ($C_{vdW} = 10^{-30}$ Nm$^3$).

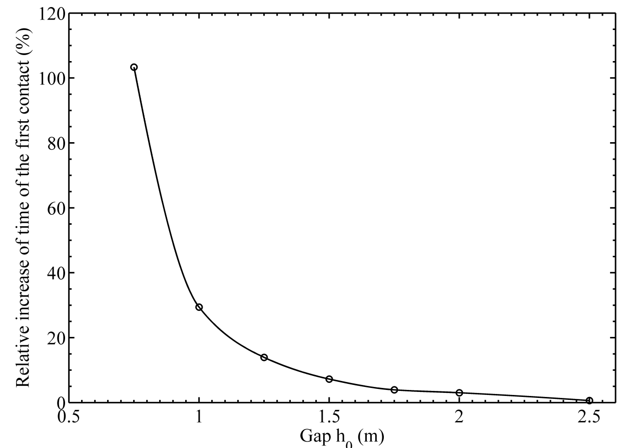


**Fig. 6.** Relative increase of time to the first contact $t_1$ (with respect to value obtained under vacuum conditions) presented as a function of $h_0$ ($C_{vdW} = 10^{-30}$ Nm$^3$).

ALE method takes this displacement into account when computing the potential field.

**Modeling of viscous air damping.**

MEMS devices often operate in ambient pressure, therefore air functions as an important working fluid. The influence of fluids in MEMS devices manifests as viscous damping. As gas, such as air, fills the space between MEMS components, viscous air damping strongly affects the dynamic behavior of these devices. Viscous air damping can be divided into two categories: squeeze-film damping and slide-film damping. The former occurs when a micromechanical structure is pushed towards a rigid surface with a thin fluid film in between (as in microswitch), while the latter mainly occurs in horizontally moving devices (e.g. comb-drives) [1]. Nonlinear compressible isothermal Reynolds equation is used for modeling of squeeze-film damping in the case of the microswitch:

$$\frac{\partial}{\partial x}\left(h^3 P \frac{\partial P}{\partial x}\right) + \frac{\partial}{\partial y}\left(h^3 P \frac{\partial P}{\partial y}\right) = 12\mu_{eff}\left(h\frac{\partial P}{\partial t} + P\frac{\partial h}{\partial t}\right), \quad (7)$$

$$\mu_{eff} = \frac{\mu}{1 + 9.638\left(\dfrac{L_0 P_a}{p_0 h_0}\right)^{1.159}}. \quad (8)$$

where pressure in the gap $P$ and the gap thickness $h$ are functions of time and position ($x$, $y$). $\mu$ is the dynamic viscosity of the gas, $\mu_{eff}$ is effective viscosity coefficient, which is used to account for gas rarefaction effects, $p_0$ is working pressure in the gap, $L_0$ is the mean free path of air particles at atmospheric pressure $P_a$, and $h_0$ is initial gap height. For the $P_a = 101325$ Pa, $L_0 \approx 65$ nm [1,2,22]

.

**Numerical analysis of contact bouncing**

In this paper, original bi-metal complex-shaped cantilever microstructure of the microswitch is treated as an ideal homogeneous cantilever, presented in Fig. 2, with characteristic parameters indicated in Table 1. Due to symmetry only half of the microstructure is considered. In order to study contact bouncing, contact surface (representing the drain) was placed at the same level as the lower surface of the microstructure (i.e. at the initial position the microstructure was resting on the substrate). Free end of microstructure was deflected upwards by 2.0 μm and released thus forcing the tip of the microstructure to contact substrate and bounce. The simulation has been performed with zero structural damping. The aim of the numerical analysis was to determine the influence of ambient air pressure and adhesion forces on free impact vibrations.

The magnitude of squeeze-film damping in the system is determined by the ambient pressure $p_0$ and air-film thickness $h_0$. In order to study influence of air damping in the case of vibro-impact interaction of the moving microstructure with the stationary structure, two series of transient simulations were carried out. In the first one, pressure $p_0$ was varied and the rest of system parameters were kept constant. Fig. 3 illustrates numerical results, which were obtained with initial deflection of $z_0 = 2$ μm. The presented plots indicate that for the case of $h_0 = 2$ μm and $p_0 = 10 \div 100$ kPa, ambient air generates an appreciable amount of damping. The relative reduction of the first bounce amplitude $z_{max}$ at $p_0 = 10$ kPa and $p_0 = 100$ kPa with respect to vacuum conditions is equal to 6 % and 15 % respectively. While, in pressure range of $p_0 = 0.01 \div 1$ kPa the obtained values of bounce amplitude $z_{max}$ are close to each other and indicate insignificant difference in comparison to vacuum conditions.

In the second series of transient simulations ambient pressure was fixed at $p_0 = 100$ kPa, while air-film thickness was varied in the range of $h_0 = 0.75 \div 2.5$ μm. Obtained results are summarized in Fig. 4. In this case the influence of squeeze-film damping on the contact bouncing behavior is much more pronounced in comparison to the previous case. As Fig. 5 demonstrates, the amplitude of the first contact bounce $z_{max}$ reduces dramatically as the gap with

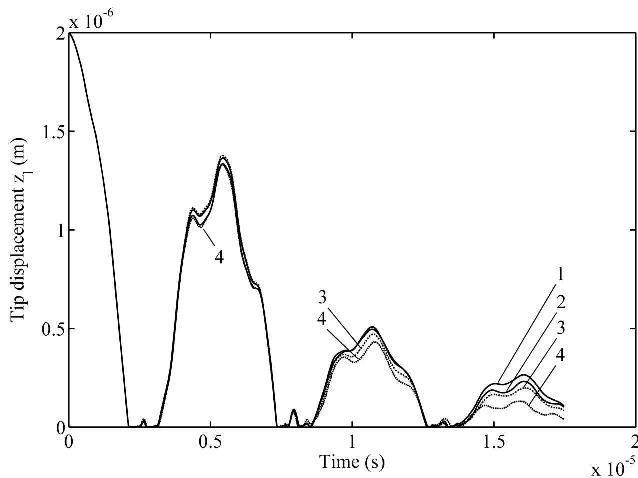


**Fig. 7.** Free impact vibrations for different $C_{vdW}$ in vacuum: 1 - $C_{vdW} = 0$, 2 - $10^{-32}$ Nm$^3$, 3 - $10^{-30}$, 4 - $10^{-27}$.

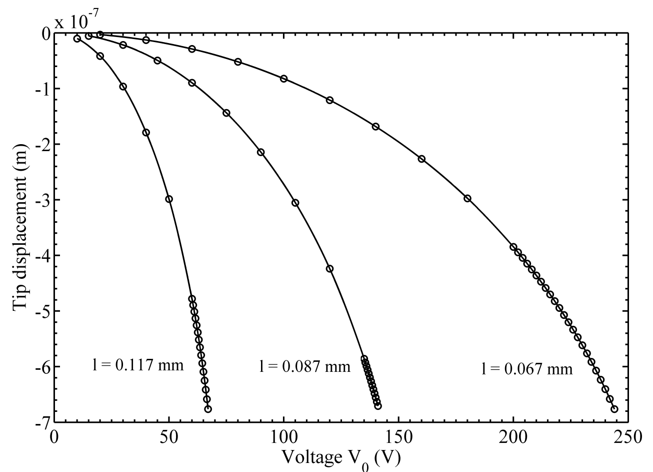


**Fig. 8.** Vertical microstructure tip displacement at different applied voltages $V_0$ for microstructures of different length $l$.

air reduces in size and for the $h_0$ = 0.75 μm the bounce amplitude $z_{max}$ is by more than 90% lower than the value obtained under vacuum conditions. One more obvious effect of reduced air-film thickness is the increase of the time to the first contact $t_1$. As the Fig. 6 indicates the increase of $t_1$ becomes particularly significant for $h_0 < 1.25$ μm.

Proposed vibro-impact model may be used to estimate contact bouncing characteristics as a function of adhesion-related parameter $C_{vdW} = A_h A_c / 6\pi$ and geometry of the microstructure. Value of contact area $A_c$ for fabricated microswitches is calculated by taking into account total area of two contact tips, which is equal to 32 μm$^2$. However, this parameter, in general, can acquire fairly different values if we consider microswitches fabricated by different research groups. Literature survey revealed that contact area of different real-life microswitches is in the range of $A_c = 0.1 \div 10^4$ μm$^2$. If we insert these values into expression for $C_{vdW}$ we obtain that the range of interest for adhesion-related parameter is $C_{vdW} = 10^{-27} \div 10^{-32}$ Nm$^3$. In order to estimate the effect of $C_{vdW}$ on dynamic response of the system, a series of simulations were performed, which results are illustrated in Fig. 7. We may observe that variation of this parameter does not have significant influence on the first bounce amplitude $z_{max}$, which is nearly coincidental for different values of $C_{vdW}$. However, influence of adhesion forces becomes more pronounced with each subsequent bounce. Bouncing reduces more rapidly for larger values of $C_{vdW}$, corresponding to larger adhesive forces.

## Numerical analysis of electromechanical coupling

One of the most important microswitch performance characteristics is the so-called pull-in voltage $V_{PI}$, which indicates the smallest voltage that can close the microswitch. A series of simulations were performed in Comsol in order to predict $V_{PI}$ of fabricated microswitches and to analyze the influence of various system parameters on the magnitude of $V_{PI}$. The values of parameters used for the numerical analysis are as follows: $l$ = 67 μm, 87 μm, 117 μm and $l_g$ = 30 μm, 50 μm, 80 μm respectively, $h_0$ = 2 μm, $h_d$ = 1 μm, while other analysis parameters are the same as listed in Table 1. In order to determine values of pull-in voltage for microswitches a parametric solver is used, which scans over a range of applied voltages $V_0$ in predefined steps and thereby computes the microstructure deflection corresponding to each voltage value. When the program tries to solve for a voltage level higher than the pull-in voltage, the solution ceases to converge since ALE technique in static mode cannot handle unstable part of microstructure deflection, which corresponds to microstructure collapsing to the bottom electrode. Thus the static simulation stops at the last converged solution, which in turn is used to determine the $V_{PI}$ (see Fig. 8). Predicted pull-in voltages are compared against results of electrical measurements (Table 2), which are discussed in the next section. This comparison indicates that simulation results are on average by 10 % larger than experimental ones. This discrepancy is not surprising because there are a number of MEMS-specific error sources, which may reduce the accuracy of results of the Comsol model: (a) Uncertainty in material properties. The model uses Young's modulus of bulk nickel (207 GPa), however, it is well-known that material properties of microfabricated materials can strongly deviate from bulk-material values and are very dependent on particular fabrication process as

Table 2. Comparison of simulated and measured pull-in voltages of fabricated microswitches.

| Length of cantilever microstructure (μm) | Pull-in voltage $V_{PI}$ (V) | | Relative error (%) |
|---|---|---|---|
| | Simulated value | Experimental value | |
| 67 | 244.70 | 226.70 | 7.94 |
| 87 | 141.10 | 128.40 | 9.89 |
| 117 | 67.30 | 59.90 | 12.35 |

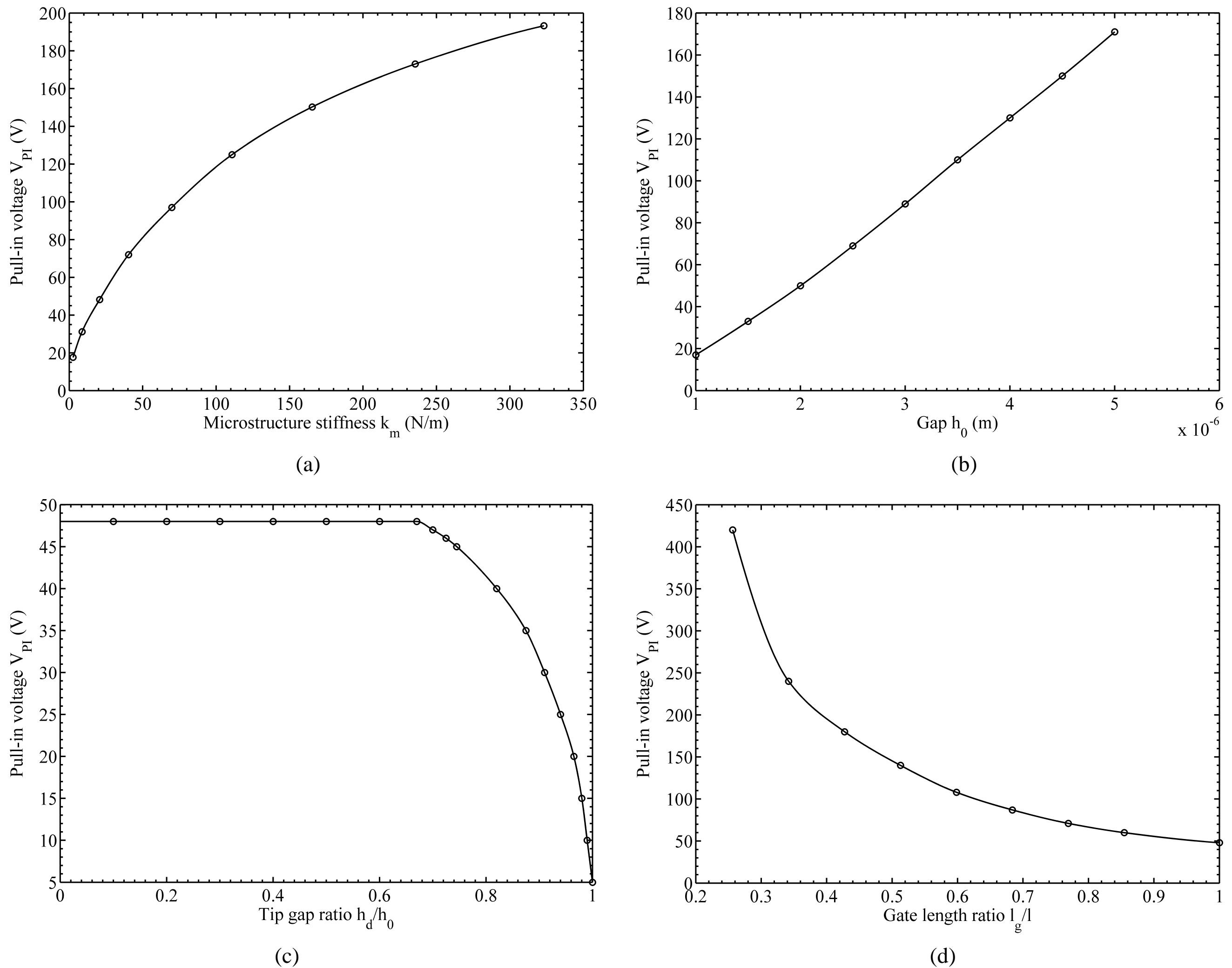


**Fig. 9.** Variation of simulated pull-in voltage of a microswitch $V_{PI}$ as a function of different system parameters.

well as its technological parameters [1]. For example, mechanical properties of electroplated nickel strongly depend on current density used for deposition. In literature we may find large variations in experimental values of Young's modulus of thin-film nickel from different authors: e.g. in [1] – 200 GPa and in [23] – 160 GPa; (b) Uncertainty in geometric dimensions. $V_{PI}$ is especially sensitive to variation of microstructure thickness $t$ since cantilever stiffness is proportional to $t^3$, and the thickness is that particular parameter of the microstructure which is very prone to variations due to microfabrication errors associated with variations in nickel electroplating duration and current density; (c) Structural and anchoring idealizations. In the Comsol model the actual microstructure of the fabricated microswitches is approximated by a homogeneous microstructure having ideal cantilever-type fixing conditions. However it is well known in MEMS community that fixing conditions of microfabricated beams at the anchors usually deviate from ideal boundary conditions. Real, non-ideal anchors have either so-called step-up or cup-shaped profile that allow for more rotation and stress absorption, which in turn results in increased anchor compliance and therefore reduces microstructure stiffness [24]. Consequently this leads to lower experimental values of pull-in voltages.

Value of pull-in voltage depends on and may be controlled by a number of system parameters including: microstructure stiffness $k_m$, nominal gap thickness $h_0$, tip gap $h_d$, overlap area between the gate and the microstructure $A_g$ and gate length $l_g$. A series of finite element simulations were carried out with the Comsol model in order to conduct a parametric study for determination of dependences of pull-in voltage on aforementioned parameters. Fig. 9(a) presents the evolution of pull-in voltage with respect to a wide range of values of microstructure stiffness $k_m$. The purpose of this numerical analysis was to modify only structural characteristics of the microsystem therefore value of $k_m$ was changed by varying microstructure thickness $t$ because variation of length or width also changes magnitude of electrostatic forces since these geometric parameters simultaneously affect not only structural stiffness but also the size of overlap area $A_g$ and the relative position of gate electrode. It is obvious from the obtained characteristic in

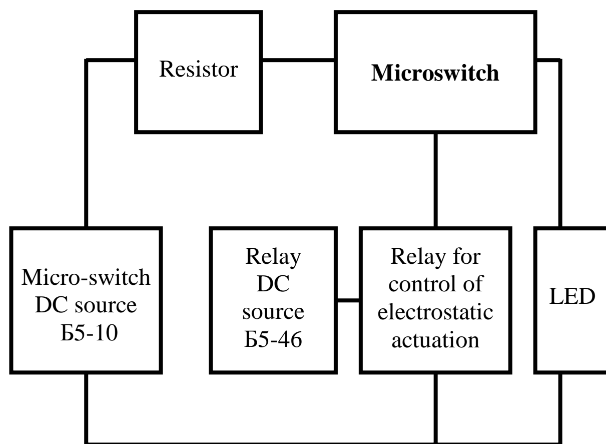


**Fig. 10.** Block diagram of measurement setup used for electrical characterization of fabricated microswitches**.**

Fig. 9(a) that for stiffer structure a larger voltage is needed in order to bend it. Thus, desired value of microswitch pull-in voltage may be achieved by tuning microstructure stiffness, which may be altered by adjusting geometric dimensions of the microstructure, modifying its shape and configuration as well as selecting different materials for fabrication. The variation of pull-in voltage for different values of initial gap $h_0$ is illustrated in Fig. 9(b). In this case, only the distance between the microstructure and the gate is modified. It means that structural characteristics of the microsystem are not modified, only the electrostatic forces are increased when the gap $h_0$ is reduced resulting in lower pull-in voltages. Another structural method for reducing pull-in voltage is to introduce miniature contact tips (bumps) on the bottom side of the free end of the microstructure thereby reducing the distance that the microstructure has to be deflected until it touches the bottom electrode. The influence of height of contact tips on the value of pull-in voltage is illustrated in Fig. 9(c) in the form of relationship between $V_{PI}$ and tip gap ratio $h_d/h_0$. The shape of this plot leads to a conclusion that due to the pull-in instability phenomenon the influence of contact tips starts to manifest only when their height exceeds $2/3h_0$. It is obvious that the tips which height is larger than $2/3h_0$ have a pronounced effect in reducing pull-in voltage. The magnitude of generated electrostatic forces may be regulated by modification of the size of the gate electrode thereby changing the overlap area $A_g = l_g w$. Thus, one of the ways to achieve this is to change gate length $l_g$. The effect of different values of $l_g$ on $V_{PI}$ is demonstrated in Fig. 9(d), which indicates that reduction of overlap area dramatically raises the pull-in voltage leading to unacceptably high values for $l_g = 1/2l$ and less.

## Experimental testing of fabricated microswitches

Aim of the experimental investigation of fabricated microswitch prototypes was to carry out electrical measurements of pull-in voltage of these microdevices. They were fabricated on three substrates made from different material: silicon, quartz and sital. Each substrate contained an array of approximately 560 (20×28) devices. Due to their miniature size a special experimental setup with a microscope and probe station was used. The aim of initial experimental work was to identify those microdevices that were defective due to stiction. For this purpose resistance measurements were carried out in between source-gate and source-drain electrodes. Results of these measurements revealed that stiction of the free-end of the microstructure to the drain was a primary cause of failure of the microswitches. Furthermore, it was determined that the smallest percentage of defective microswitches was among those that were fabricated on sital substrate and had the shortest microstructure.

Electrical measurement circuit, presented in Fig. 10, was set up in order to perform electrostatic actuation experiments on microswitches and determine their pull-in voltage. For the actuation of the microswitch a DC power source Б5-10 was placed in series. Electromagnetic relay, powered by DC power source Б5-46, was inserted into the measurement circuit in order to have the possibility of switching the actuation voltage on or off during testing. In order to limit electric current flowing through closed microswitch, 10 kΩ resistor was connected in series with the microswitch. Light-emitting diode (LED) was used in order to indicate the moment when the switch is closed. The pull-in voltage was measured by: (a) applying actuation voltage by turning on the electromagnetic relay, (b) increasing gradually actuation voltage with power source Б5-10 until LED flashes and recording at this moment indications of voltage with multi-meter UNI-T M830B. Pull-in voltages were measured for microswitches of three different lengths: 67 μm, 87 μm and 117 μm. The corresponding average values of the measured pull-in voltages are listed in Table 2.

## Conclusion

This paper reports on dynamic modeling and simulation of electrostatically-actuated cantilever microstructure, which represents elastic contacting element of fabricated MEMS switches. Several FE models have been developed that account for vibro-impact interactions between the cantilever tip and the drain, influence from electrostatic field and damping due to squeezed air in the gap. For the numerical study of detrimental contact bouncing phenomenon a general adhesive-repulsive contact model has been implemented in Comsol FE software, whose adhesive contribution is represented by van der Waals force component and the repulsive contribution - by a linear elastic force. For modeling of squeeze-film damping, a compressible isothermal Reynolds equation was employed, which solves for the air pressure acting on the microstructure. For numerical analysis of switching characteristics, 3-D FE model of a flexible microstructure under the effect of nonlinear electrostatic forces was developed within Comsol.

Obtained numerical results indicate that under typical values of ambient pressure and air-film thickness,

amplitude of the first bounce is reduced by more than 90 %, while the time till the first contact is increased by more than 100 % in comparison to values obtained under vacuum conditions. Simulations revealed that intermolecular adhesive forces do not have significant influence on the magnitude of the first bounce amplitude, however the influence intensifies with each subsequent bounce. It was demonstrated that increase of adhesive forces results in more rapid reduction of bouncing.

Numerical analysis of electrostatic-structural interaction allowed prediction of pull-in voltages of fabricated microswitches. Results of parametric analysis demonstrated how value of pull-in voltage may be adjusted by modifying different system parameters.

Operation of fabricated microswitches has been tested in the experimental setup consisting of a microscope-based probe station and an arrangement of electric instrumentation. Values of pull-in voltages were measured and compared with the simulation results. Explanation of possible reasons for the obtained discrepancies was subsequently provided.

**References**

[1] **Gad-el-Hak M.** The MEMS Handbook, CRC Press, USA, 2002.

[2] **Rebeiz G.B.** RF MEMS: Theory, Design, and Technology, Wiley-Interscience, USA, 2003.

[3] **Patton S.T., Zabinski J.S.** "Failure Mechanisms of Capacitive MEMS RF Switch Contacts" Tribology Letters, Vol. 19(4), pp. 265-272, 2005.

[4] **Brown E.** "RF-MEMS Switches for Reconfigurable Integrated Circuit" IEEE Transactions on Microwave Theory and Techniques, Vol. 46(11), pp. 1868-1880, 1998.

[5] **Jensen B. D., Huang K., Chow L., Kurabayashi K.** "Adhesion Effects on Contact Opening Dynamics in Micromachined Switches" Journal of Applied Physics, Vol. 97, pp. 1-9, 2005.

[6] **Decuzzi P., Demelio G.P., Pascazio G., Zaza V.** "Bouncing Dynamics of Resistive Microswitches With an Adhesive Tip" Journal of Applied Physics, Vol. 100, pp. 1-9, 2006.

[7] **Kogut L., Komvopoulos K.** "The Role of Surface Topography in MEMS Switches and Relays" Proc. of 2004 ASME International Joint Tribology Conference, Long Beach, USA, pp. 1-5, 2004.

[8] **McCarthy B., Adams G.G., McGruer N.E., Potter D.** "A Dynamic Model, Including Contact Bounce, of an Electrostatically Actuated Microswitch" Journal of Microelectromechanical Systems, Vol. 11, pp. 276-283, 2002.

[9] **Majumder S., McGruer N.E., Adams G.G., Zavracky P.M., Morrison R.H.** "Study of Contacts in an Electrostatically Actuated Microswitch" Sensors and Actuators A, Vol. 93, pp. 19-26, 2001.

[10] **Petersen, K.** "Micromechanical Membrane Switches on Silicon" IBM Journal of Research and Development, Vol. 23, pp. 376-385, 1979.

[11] **Barauskas R., Ostasevicius V.** Analysis and Optimization of Elastic Vibro-Impact Systems, Technologija, Lithuania, 1999.

[12] **Ostasevicius V.** Elektromechaniniu Sistemu Dinamika, Technologija, Lithuania, 2000.

[13] **Maboudian R., Howe R.T.** "Critical Review: Adhesion in Surface Micromechanical Structures" Journal of Vacuum Science and Technology B, Vol. 15(1), pp. 1-20, 1997.

[14] **Bhushan B.** Springer Handbook of Nanotechnology, Springer-Verlag, Germany, 2004.

[15] **Komvopoulos K.** "Adhesion and Friction Forces in Microelectromechanical Systems: Mechanisms, Measurement, Surface Modification, Techniques, and Adhesion Theory" Journal of Adhesion Science and Technology, Vol. 17(4), pp. 477-517, 2003.

[16] **Coutu R.A., Kladitis P.E., Leedy K.D., Crane R.L.** "Selecting Metal Alloy Electric Contact Materials for MEMS Switches" Journal of Micromechanics and Microengineering, Vol. 14(8), pp. 1157-1164, 2004.

[17] **Berger E. J.** "Friction Modeling for Dynamic System Simulation" Applied Mechanics Reviews, Vol. 55(6), pp. 535-577, 2002.

[18] **Delrio F.W., De Boer M.P., Knapp J.A., et al.** "The Role of Van der Waals Forces in Adhesion of Micromachined Surfaces" Nature Materials, Vol. 4, pp. 629-634, 2005.

[19] **Tayebi N., Polycarpou A.A.** "Adhesion and Contact Modeling and Experiments in MEMS Including Roughness Effects" Microsystem Technology, Vol. 12, pp. 854-869, 2006.

[20] **Israelachvili J.N.** Intermolecular and Surface Forces, Academic Press, London, 1998.

[21] FEMLAB 3.2 MEMS Module Model Library, 2005.

[22] **Hamrock B.J., Schmid S.R., Jacobson B.O.** Fundamentals of Fluid Film Lubrication, McGraw-Hill, 2004.

[23] **Bucheit T., Christenson T., Schmale D., Lavan D.** "Understanding and Tailoring the Mechanical Properties of LIGA Fabricated Materials" Proc. of MRS Symposium, Vol. 546, pp. 121-126, 1998.

[24] **Lishchynska M., Cordero N., Slattery O., O'Mahony C.** "Modeling Electrostatic Behavior of Microcantilevers Incorporating Residual Stress Gradient and Non-Ideal Anchors" Journal of Micromechanics and Microengineering, Vol. 15, pp. 10-14, 2005.